Interference and multipath sequential tests for signal integrity in multi-antenna GNSS receivers

Daniel Egea, José A. López-Salcedo, Gonzalo Seco-Granados
Department of Telecommunications and Systems Engineering
Universitat Autònoma de Barcelona (UAB)
08193 Bellaterra, Barcelona (Spain)

***Abstract*—This paper addresses the problem of detecting external threats such as multipath and interference signals, which may compromise the integrity of Global Navigation Satellite System (GNSS) receivers. We will focus herein on multi-antenna GNSS receivers, for which detection metrics will be proposed in order to capture the change behavior of the threat under analysis. For a prompt threat detection, we adopt quickest detection techniques such as the CUSUM algorithm, and we validate their performance through numerical simulations.**

I. Introduction

With the widespread deployment of Global Navigation Satellite Systems (GNSS), one of the major challenges to be solved is the provision of integrity to users beyond the civil aviation community, where this feature is already a well-established performance criterion [1]. *Integrity* refers to the ability of the user receiver to guarantee the quality and trust of the received signal, in such a way that critical or commercial applications can be safely operated. As a matter of fact, integrity is now becoming a general concern within the GNSS community due to the widespread deployment of terrestrial GNSS receivers (e.g. embedded in most smartphones), the increasing interest in providing ubiquitous positioning, and the emergence of new GNSS-based applications and services [2].

A new approach must be taken when dealing with integrity for terrestrial GNSS techniques, since the impairments in the aviation domain are dramatically different to those of terrestrial users. Herein, we will concentrate on multipath, non-line-of-sight propagation (NLOS) and the presence of interference signals, as the major impairments that can threat the integrity of terrestrial users. Significant efforts have been made to mitigate these impairments effects using multi-antenna GNSS receivers [3], often leaving detection in background. However, the detection process is actually as important, or even more important than mitigation. The reason is that before using mitigation techniques, we need to know whether some impairment is present or not. Otherwise, the effects of mitigation techniques could seriously damage the GNSS signal of interest.

Most of the current detection approaches adopt a classical detection framework [4], [5], focusing on detection probability. A feature of these schemes is that detection is carried out in a block-wise manner, where a set of samples are processed before a decision is done. Nonetheless, for integrity monitoring purposes, the detection delay is also a critical performance parameter, since we are interested on detecting the threats as soon as possible. This is the underlying concept of quickest detection, a sequential detection framework whose most popular technique is the cumulative sum (CUSUM) algorithm [6].

The application of the CUSUM algorithm to multi-antenna receivers has been explored so far [7]. Nevertheless, to the best of the authors' knowledge, the CUSUM has not been used yet for integrity monitoring. Based on this observation, the goal of this work is to apply the CUSUM for interference and multipath detection in multi-antenna GNSS receivers with aim of improving its integrity. For the interference case, we exploit the idea of the eigenvalue ratio test used in cognitive radio for spectrum sensing [8]. For the multipath case, the suggested approach relies on the comparison between the expected steering vector and the one actually being received. To do so, the direction-of-arrival (DoA) of the line-of-sight (LOS) GNSS signals must be known in advance. This is possible because the position of visible satellites is already computed within any GNSS receiver, and the DoA can be obtained using the antenna array and the user attitude from external sensors

The rest of this paper is organized as follows. Section II introduces the signal model and Section III the CUSUM algorithm and the proposed metrics for interference and multipath detection. In Section IV, numerical results are presented to evaluate the proposed detection techniques, and conclusions are drawn in Section V.

II. Signal model

Let us consider an antenna array composed of a uniform linear array (ULA) with N_a antenna elements spaced at a distance d. For an incident signal with DoA θ, the array response or steering vector has the following form:

$$\mathbf{s}(\theta) = \left[1 \quad e^{j2\pi(d/\lambda)\cos(\theta)} \cdots e^{j(N_a-1)2\pi(d/\lambda)\cos(\theta)}\right]^T, \qquad (1)$$

where λ is the wavelength. The noise at each antenna is modeled as an i.i.d zero-mean complex Gaussian random process with variance σ_w^2, and uncorrelated both spatially and temporally. Two different signal models will be considered for either interference or multipath detection, as described next.

A. Interference detection signal model

Detection is carried out here before the GNSS correlation. In the absence of interference, the received signal at each antenna will be dominated by noise (since the GNSS signal remains under the noise floor), whereas in the presence of interference, the received signal will be dominated by the interference itself. The detection problem thus becomes:

$$\begin{aligned}\mathcal{H}_0 &: \mathbf{r}(n) = \mathbf{w}(n)\\ \mathcal{H}_1 &: \mathbf{r}(n) = i(n)\cdot\mathbf{s}(\theta_t) + \mathbf{w}(n)\end{aligned} \qquad (2)$$

where $\mathbf{r}(n) \doteq [r_1(n), \cdots, r_{N_a}(n)]^T$ contains the discrete-time baseband complex samples of the N_a antennas at time n, $i(n)$ models an interference signal with DoA θ_t and $\mathbf{w}(n)$ is the noise vector disturbing the received samples.

B. Multipath detection signal model

Detection is carried out at the GNSS correlator output, since it is here where the GNSS signal and multipath effects actually become

This work was partly supported by the Spanish Government under grant TEC2011-28219 and by the Catalan Government under grant 2009 SGR 298.

visible. We use a single correlator output centered at the correlation peak (i.e. the prompt correlator). The received signal becomes:

$$\begin{aligned} \mathcal{H}_0 &: \mathbf{y}(m) = \alpha_0 \cdot \mathbf{s}(\theta_s) + \mathbf{e}(m) \\ \mathcal{H}_1 &: \mathbf{y}(m) = \alpha_0 \cdot \mathbf{s}(\theta_s) + \alpha_1 \cdot \mathbf{s}(\theta_t) + \mathbf{e}(m) \end{aligned} \tag{3}$$

where $\mathbf{y}(m) \doteq [y_1(m), \cdots, y_{N_a}(m)]^T$ contains the post-correlation outputs of each of the N_a signals at time m, whereas θ_s and θ_t are the LOS and multipath signal DoA, respectively. The complex amplitude α_j with $j = \{0, 1\}$, corresponds the LOS and multipath signal post-correlation components, respectively. Finally, $\mathbf{e}(m)$ is the post-correlation zero-mean complex Gaussian noise with variance σ_e^2.

III. Sequential Tests for Integrity Monitoring

A. Fundamentals of sequential detection

For the prompt detection of integrity threats, it is essential to formulate the problem under the framework of sequential change detection [9]. To do so, let us first consider a set of observations $\mathbf{x} = [x(0), x(1), \ldots, x(K-1)]^T$ that follow a statistical distribution $f_0(\mathbf{x})$ under $\mathcal{H}_0$, and change to a different distribution $f_1(\mathbf{x})$ under $\mathcal{H}_1$. Thus, sequential change detection aims at finding a strategy that minimizes the detection delay $\overline{T}_1$, while keeping the mean time between false alarms $\overline{T}_0$ larger than a conveniently set value N_{FA}.

The CUSUM algorithm is a simple but efficient sequential change detection algorithm, based on the log likelihood ratio (LLR) of the densities before and after the change, $f_0(\mathbf{x})$ and $f_1(\mathbf{x})$. That is $\mathrm{LLR}(\mathbf{x}) \doteq \ln(f_1(\mathbf{x})/f_0(\mathbf{x}))$. The CUSUM algorithm was first proposed in [6] as a decision test comparing

$$g(k+1) = [g(k) + \mathrm{LLR}(x(k+1))]^+ \tag{4}$$

with a given threshold h, where $[x]^+ \doteq \max\{0, x\}$. Hence, it is possible to compute $g(k)$ recursively by setting $g(0) = 0$, and then an alarm is raised whenever $g(k+1) > h$.

From [9], it is known that the CUSUM algorithm minimizes $\overline{T}_1$ among all detection algorithms that satisfy $\overline{T}_0 \geqslant N_{\mathrm{FA}}$. Then, it is possible to derive some approximations for $\overline{T}_0$ with the aim of finding the threshold h that guarantees a given false alarm rate N_{FA}:

$$\overline{T}_0 \geqslant e^h = N_{\mathrm{FA}}. \tag{5}$$

B. Interference detection

The spatial correlation matrix $\mathbf{R}_{rr} \doteq E\left[\mathbf{r}\mathbf{r}^H\right]$ will be used herein to obtain a change detection metric, since it shows a clearly different behavior in the presence of interference signals, as inferred from (2). Specifically, under $\mathcal{H}_0$, all the eigenvalues of $\mathbf{R}_{rr}$ are equal to σ_w^2. However, under $\mathcal{H}_1$ the eigenvalues are different, with $\lambda_{\max}|_{\mathcal{H}_1} = P_{int}N_a + \sigma_w^2$ and $\lambda_{\min} = \sigma_w^2$. It is then clear that when no interference is present, $\frac{\lambda_{\max}}{\lambda_{\min}}|_{\mathcal{H}_0} \approx 1$, whereas for any interference (even with low power), $\frac{\lambda_{\max}}{\lambda_{\min}}|_{\mathcal{H}_1} = 1 + N_a\mathrm{INR} > 1$, with $\mathrm{INR} \doteq P_{int}/\sigma_w^2$ the received interference-to-noise-ratio. This fact, and results in [8], suggest that the following observations could be fed to the CUSUM algorithm for the sake of change detection:

$$x_{\mathrm{i}}(k) \doteq \frac{\hat{\lambda}_{\max}(k)}{\hat{\lambda}_{\min}(k)} \tag{6}$$

where the subscript $_{\mathrm{i}}$ denotes observations for *interference* detection. To obtain these observations, the receiver can estimate the spatial correlation matrix based on a set of N_{sp} snapshots of $\mathbf{r}(n)$ as follows,

$$\hat{\mathbf{R}}_r(k) \doteq \frac{1}{N_{sp}} \sum_{n=0}^{N_{sp}-1} \mathbf{r}(n - kN_{sp})\mathbf{r}^H(n - kN_{sp}) \tag{7}$$

and then computes the maximum and minimum eigenvalue of each $\hat{\mathbf{R}}_r(k)$, denoted by $\hat{\lambda}_{\max}(k)$ and $\hat{\lambda}_{\min}(k)$.

With the goal of applying the CUSUM algorithm to $x_{\mathrm{i}}(k)$, we first need to know its statistical distribution, as required in (4). A useful result here is the Gaussian approximation for the distribution of extreme eigenvalues, for even low N_{sp} [10], whereby $x_{\mathrm{i}}(k)_{\mathcal{H}_0} \sim \mathcal{N}(A_{0,\mathrm{i}}, \sigma_{0,\mathrm{i}}^2)$ with

$$A_{0,\mathrm{i}} \doteq \mathrm{E}_{\mathcal{H}_0}\left[\frac{\hat{\lambda}_{\max}}{\hat{\lambda}_{\min}}\right] \approx \frac{a_1 - 1.771 b_1}{a_K - 1.771 b_K}, \tag{8}$$

$$\sigma_{0,\mathrm{i}}^2 \doteq \mathrm{var}_{\mathcal{H}_0}\left[\frac{\hat{\lambda}_{\max}}{\hat{\lambda}_{\min}}\right] \approx \frac{b_1^2}{N_{sp} b_K^2} \tag{9}$$

and constants $a_{\substack{1\\K}}$, $b_{\substack{1\\K}}$ given by

$$a_{\substack{1\\K}} \doteq \left(\sqrt{N_a} \pm \sqrt{N_{sp}}\right)^2, \tag{10}$$

$$b_{\substack{1\\K}} \doteq \left(\sqrt{N_a} \pm \sqrt{N_{sp}}\right)\left(\sqrt{\frac{1}{N_a}} \pm \sqrt{\frac{1}{N_{sp}}}\right)^{1/3}. \tag{11}$$

Therefore, we can formulate the change detection problem as:

$$\begin{aligned} \mathcal{H}_0 &: x_{\mathrm{i}}(k) \sim \mathcal{N}\left(A_{0,\mathrm{i}}, \sigma_{0,\mathrm{i}}^2\right) \\ \mathcal{H}_1 &: x_{\mathrm{i}}(k) \sim \mathcal{N}\left(A_{1,\mathrm{i}}, \sigma_{0,\mathrm{i}}^2\right) \end{aligned} \tag{12}$$

where $A_{1,\mathrm{i}} \doteq \mathrm{E}_{\mathcal{H}_1}\left[\frac{\hat{\lambda}_{\max}}{\hat{\lambda}_{\min}}\right] \approx 1 + N_a\mathrm{INR}$ and, in a first approach, the same variance is assumed before and after the change. This leads to the so-called only-mean change (MC) problem. The CUSUM algorithm can thus be applied, whose recursion is based on the following MC-LLR [9]:

$$\mathrm{LLR}_{\mathrm{MC}}(x_{\mathrm{i}}(k)) = \frac{A_{1,\mathrm{i}} - A_{0,\mathrm{i}}}{\sigma_{0,\mathrm{i}}^2}\left(x_{\mathrm{i}}(k) - \frac{A_{1,\mathrm{i}} + A_{0,\mathrm{i}}}{2}\right). \tag{13}$$

It is important to note that $\frac{\hat{\lambda}_{\max}}{\hat{\lambda}_{\min}}|_{\mathcal{H}_1}$ is known to be larger than some value, which depends on the INR. Hence, a way to proceed is to fix a certain value for $\frac{\hat{\lambda}_{\max}}{\hat{\lambda}_{\min}}|_{\mathcal{H}_1}$ according to the minimum INR that one expects to detect, denoted by ρ (i.e. the detector sensitivity) and used to fix $A_{1,\mathrm{i}}$. In this way, a minimum change detection is set allowing the detection of any larger change caused by higher power interferences. However, the finite length estimation of extreme eigenvalues can incur in estimation errors that eventually mask the interference effects on $\hat{\lambda}_{\max}$, thus causing $\mathcal{H}_1$ to be the same as $\mathcal{H}_0$, and hence nullifying the change behavior of the eigenvalue ratio test. To avoid this issue, the number of snapshots N_{sp} is set in such a way that ρ is always greater than ρ_{crit}, which is possible in virtue of the following result [11]:

$$\rho > \rho_{\mathrm{crit}} = \frac{1}{\sqrt{N_a N_{sp}}}. \tag{14}$$

A more realistic approach to the equal variance assumption in (12) can be followed by using the results in [10], where it is shown how the variance under $\mathcal{H}_1$ actually depends on the INR, being different from the one under $\mathcal{H}_0$. Reformulating the LLR required in (4) under this variance-and-mean change (VMC) problem, we get:

$$\mathrm{LLR}_{\mathrm{VMC}}(x_{\mathrm{i}}(k)) = \ln\left(\frac{\sigma_{0,\mathrm{i}}}{\sigma_{1,\mathrm{i}}}\right) + \frac{(x_{\mathrm{i}}(k) - A_{0,\mathrm{i}})^2}{2\sigma_{0,\mathrm{i}}^2} - \frac{(x_{\mathrm{i}}(k) - A_{1,\mathrm{i}})^2}{2\sigma_{1,\mathrm{i}}^2} \tag{15}$$

where $\sigma_{1,\mathrm{i}}^2 = \frac{(N_a\rho+1)^2+1}{N_{sp}}$.

C. Multipath detection

In order to obtain the required observations for the CUSUM algorithm, we will first obtain $\mathbf{z}(m) \doteq \mathbf{y}(m) \odot \mathbf{s}^*(\theta_s)$ with $\odot$ the Schur-Hadamard product. By doing so, we remove the effects of the desired signal and obtain a reference signal that provides us information on the presence of multipath. This can be observed by taking a look at the resulting signal model:

$$\begin{aligned} \mathcal{H}_0 &: \mathbf{z}(k) = \alpha_0 \mathbf{1}_{N_a} + \mathbf{e}(k) \\ \mathcal{H}_1 &: \mathbf{z}(k) = \alpha_0 \mathbf{1}_{N_a} + \alpha_1 \left[\mathbf{s}\left(\theta_t\right) \odot \mathbf{s}^*\left(\theta_s\right)\right] + \mathbf{e}(k) \end{aligned} \tag{16}$$

with $\mathbf{1}_{N_a}$ a $(N_a \times 1)$ all-ones vector. Based on $\mathbf{z}(k)$, the following scalar observations are proposed for implementing the CUSUM algorithm:

$$x_{\mathrm{mp}}(k) = \frac{1}{N_a - 1} \sum_{n=2}^{N_a} \left([\mathbf{z}(k)]_n - [\mathbf{z}(k)]_1 \right) \tag{17}$$

where $[\mathbf{z}(k)]_j$ indicates the j-th component of $\mathbf{z}(k)$. This expression denotes the average of the differences between antenna pairs, once the LOS steering vector has been removed. In the absence of multipath the result is expected to be negligible, since $[\mathbf{z}(k)]_n$ is the same for all antennas. However, in the presence of multipath it contains the different contribution of multipath in different antennas, and thus multipath becomes detectable.

For implementing the CUSUM algorithm on the observations $x_{\mathrm{mp}}(k)$, based on (16) we can assume that they are Gaussian distributed with

$$A_{0,\mathrm{mp}} \doteq \mathrm{E}_{\mathcal{H}_0}\left[x_{\mathrm{mp}}(k)\right] = 0, \tag{18}$$

$$\sigma^2_{0,\mathrm{mp}} \doteq \mathrm{var}_{\mathcal{H}_0}\left[x_{\mathrm{mp}}(k)\right] = \frac{2\sigma_e^2}{N_a - 1} \tag{19}$$

when multipath is absent. When a deterministic multipath ray is present, we will have

$$A_{1,\mathrm{mp}} \doteq \mathrm{E}_{\mathcal{H}_1}\left[x_{\mathrm{mp}}(k)\right] = \frac{\alpha_1}{N_a - 1} \cdot \sum_{n=1}^{Na-1} \left(e^{j\omega(\theta_t,\theta_s)n} - 1 \right) \tag{20}$$

with $\omega(\theta_t, \theta_s) \doteq 2\pi\frac{d}{\lambda}\left(\cos(\theta_t) - \cos(\theta_s)\right)$. Therefore, we can formulate the change detection problem as:

$$\begin{aligned} \mathcal{H}_0 &: x_{\mathrm{mp}}(k) \sim \mathcal{N}\left(0, \sigma^2_{0,\mathrm{mp}}\right) \\ \mathcal{H}_1 &: x_{\mathrm{mp}}(k) \sim \mathcal{N}\left(A_{1,\mathrm{mp}}, \sigma^2_{0,\mathrm{mp}}\right) \end{aligned} \tag{21}$$

While $\sigma^2_{0,\mathrm{mp}}$ can easily be obtained in practice, $A_{1,\mathrm{mp}}$ depends on the amplitude and DoA of the multipath ray, and thus it remains unknown. The solution here is to replace the unknown parameter by its maximum likelihood estimate, leading to the generalized likelihood ratio (GLR) CUSUM algorithm. For a change in the mean of an independent Gaussian sequence, it leads to [9]:

$$g_{\mathrm{GLR}}(k) = \frac{1}{2\sigma^2_{0,\mathrm{mp}}} \max_{1 \leqslant n \leqslant k} \frac{1}{k - n + 1} \left[\sum_{i=n}^{k} \left| x_{\mathrm{mp}}(k) - A_{0,\mathrm{mp}} \right|^2 \right] \tag{22}$$

with $A_{0,\mathrm{mp}}$ being equal to 0 in our case. Finally, it is possible to fix the threshold to $h = -\ln(a/b)$, with $b = 3\ln(\gamma^{-1})$ assuring that:

$$\overline{T}_0 \geqslant \gamma^{-1} = N_{\mathrm{FA}}. \tag{23}$$

IV. Simulation Results

A. Interference detection results

We will compare first the performance of the proposed MC test in (13) and the VMC test in (15), in terms of detection delay and samples between false alarms. An antenna array using $N_a = 3$ and $d = \lambda/2$ is considered, with $\theta_t = \pi/8$. The simulation is obtained tuning the CUSUM parameters with the expressions in Section III-B, fixing a minimum detectable $\rho = -10$ dB, and using (4). The value $\rho = -10$ dB assures the detection of most GNSS interferences, whose power levels are typically higher than the receiver noise power. This can be seen in Table I, which shows the maximum and minimum expected INR among the most common interference sources [12], assuming free-space propagation and a noise level of -111 dBm (expected in a commercial GPS receiver with a 2 MHz bandwidth at room temperature).

TABLE I
Maximum and minimum GNSS INR for the simulation analysis

Service	P_{TX}	f_0	dist.	P_{RX}	INR
Radionavigation	24 kW	1250 MHz	10 km	-40.5 dB	70.4 dB
Amateur Radio	10 W	1350 MHz	25 km	-83.0 dB	28.0 dB

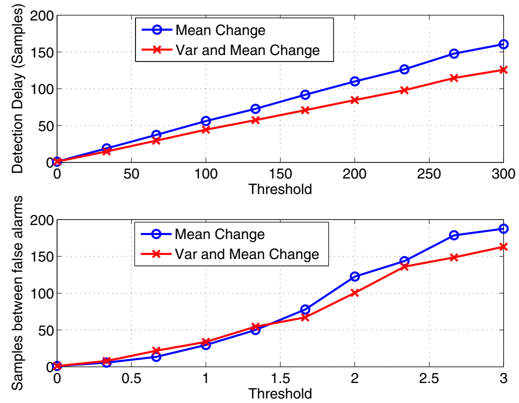

Fig. 1. CUSUM performance vs detection threshold h. Detection delay (up) and time between false alarms (down), are both measured in samples.

The results in Fig. 1 show a lower detection delay for the VMC test compared to the MC, since the former uses more information and has a more accurate model than the latter. Regarding the samples between false alarms, the bottom plot in Fig. 1 shows a zoomed representation for $h \in [0, 3]$, where the VMC seems to have slightly more frequent false alarms than the MC. However, this difference becomes negligible for higher thresholds, (not shown here due to the exponentially increasing time required to find false alarm events for large thresholds), while the difference in the detection delay increases linearly with the threshold and is in favor of the VMC. Hence, for the interference detection problem under study, the performance of the VMC test is found to be better than the MC test.

Fig. 2 shows the performance as a function of the mismatch between the true value of $A_{1,\mathrm{i}}$ and the one actually tuned in the LLR. It can be seen that the detection delay is reduced as the true value increases with respect to the tuned value. This is expected to be our case in practice, since we tune the LLR according to a minimum detectable INR. However, care must be taken when this minimum value approaches $A_{0,\mathrm{i}}$, since a high false alarm rate is incurred (i.e. lower samples between false alarms). Thus, instead of fixing $A_{1,\mathrm{i}}$ to a very low value that may never occur, it is preferable to leave some distance with respect to $A_{0,\mathrm{i}}$ (e.g. around 25 dB in our case) in order to still have a good delay detection but keeping the false alarm rate low. Another observation that can be extracted from Fig. 2 is that for large mismatches, both the MC and VMC tests provide similar performance both in false alarm and detection delay.

B. Multipath detection results

A correlation time of 1 ms is assumed here for receiver operating at $C/N_0 = 45$ dB-Hz. In order to illustrate the difficulty in characterizing the change mean $A_{1,\mathrm{rm}}$ in (20), the upper and lower plots in Fig. 3 show this mean for different code-delays of the multipath ray and different signal-to-multipath ratios (SMR). Moreover, five randomly chosen carrier phases have been considered on the amplitude of the multipath ray α_1. The results evidence the complexity in selecting a

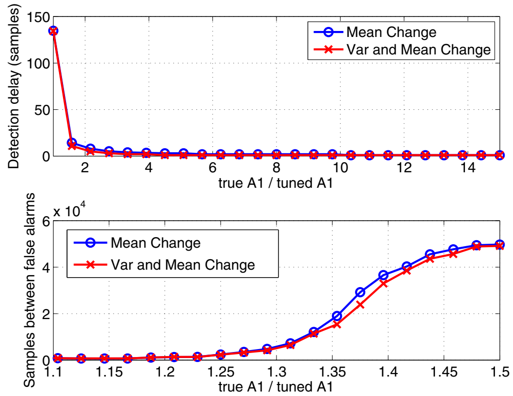

Fig. 2. Performance sensitivity to the mismatch of the tuned A_1. Detection delay for $h = 500$ (up) and time between false alarms for $h = 5$ (down).

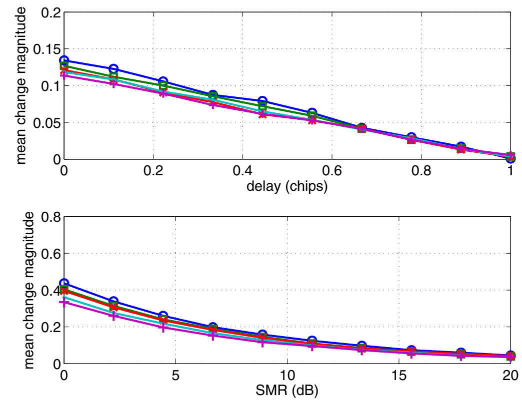

Fig. 3. Sensitivity of $|A_{1,\mathrm{mp}}|$ as a function of multipath delay at SMR=10dB (up) and SMR at 0.1 chips delay (down) for $\theta_t = 20°$ and $\theta_s = 95°$.

minimum change magnitude as it was done in the case of interference detection. This is because depending on the multipath phase and its DoA with respect to the LOS, the change magnitude will take different values even for a fixed multipath delay and SMR.

This issue motivates the adoption of the GLR CUSUM, whose performance is shown in Fig. 4. The results are obtained for a fixed multipath delay of 0.1 chips and a SMR of 10 dB. The multipath phase is chosen so as to produce the maximum and minimum change magnitude according to Fig. 3. The measured false alarm rate shown in the bottom plot of Fig. 4 is very similar for all tested magnitude changes and always remains above the lower bound in (23). The upper bound would correspond to the CUSUM expression in (5), which assumes all the parameters to be known, and it is represented by the dashed line in the bottom plot of Fig. 4 for a zoomed interval of $h \in [0, 8]$. The upper plot in Fig. 4 shows the best and worst detection delay depending on the multipath phase. Dotted lines represent the results obtained with the CUSUM algorithm assuming all parameters to be known. It can hardly be seen, but the results almost coincide for both GLR and classical CUSUM. However this doesn't mean that both algorithms have the same performance, since the time between false alarms is greater for the classical CUSUM than for the GLR, for the same threshold. In other words, to obtain the same time between false alarms as in the classical case, the GLR needs a higher threshold as observed in the bottom plot of Fig. 4, thus leading to a higher (i.e. worse) detection delay. This is the penalty incurred due to the unknown $A_{1,\mathrm{mp}}$, but it just involves a few tens of samples, and it is more than acceptable in most practical applications.

V. Conclusion

Sequential tests for interference and multipath detection in multi-antenna GNSS receivers have been investigated under the framework of quickest detection theory. The use of the proposed detectors allows the provision of signal integrity to GNSS users, allowing the user to know when the GNSS signal quality and trust are being threatened by interference or multipath, which are the major impairments in terrestrial GNSS receivers. For interference detection, both the MC and VMC CUSUM tests have been proposed by using a fixed minimum detectable INR. For multipath detection, the uncertainty regarding the multipath ray (i.e. phase, delay and relative DoA), lead us to propose a GLR CUSUM that implements the maximum likelihood estimation of the unknown mean change. Numerical results for both problems have been provided, showing the potential interest of these techniques in practical applications involving GNSS signal integrity monitoring.

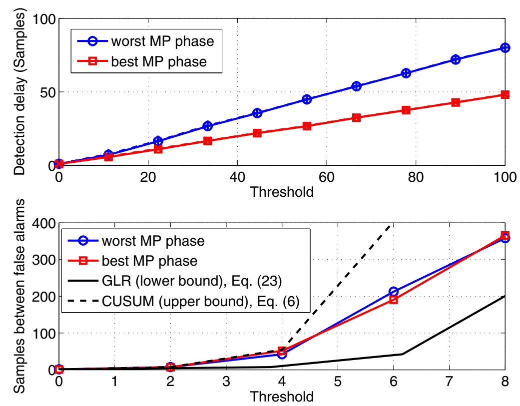

Fig. 4. GLR performance. Detection delay (up) and time between false alarms (down).

References

[1] B. W. Parkinson *et al.*, *Global Positioning System: Theory and Applications vol. 2*. Aiaa, 1996, vol. 2.

[2] G. Seco-Granados, J. A. López-Salcedo *et al.*, "Challenges in indoor global navigation satellite systems," *IEEE Signal Processing Mag.*, vol. 29, no. 2, pp. 108–131, March 2012.

[3] G. Seco-Granados *et al.*, "ML estimator and hybrid beamformer for multipath and interference mitigation in GNSS receivers," *IEEE Trans. on,Sig. Proc.*, vol. 53, no. 3, pp. 1194–1208, 2005.

[4] M. Brenneman, Y. Morton *et al.*, "GPS multipath detection with ANOVA for adaptive arrays," *IEEE Trans. on, Aeros. and Electr. Syst.*, vol. 46, no. 3, pp. 1171–1184, 2010.

[5] B. Motella *et al.*, "GNSS interference detector based on Chi-square Goodness-of-fit test," in *IEEE 2012 6th ESA Workshop on Sat. Nav. Tech. (NAVITEC)*, pp. 1–6.

[6] E. Page, "Continuous inspection schemes," *Biometrika*, pp. 100–115, 1954.

[7] L. Lai, Y. Fan, and H. V. Poor, "Quickest detection in cognitive radio: A sequential change detection framework," in *IEEE GLOBECOM*, 2008, pp. 1–5.

[8] B. Nadler *et al.*, "Performance of eigenvalue-based signal detectors with known and unknown noise level," in *IEEE ICC*, 2011, pp. 1–5.

[9] M. Basseville *et al.*, *Detection of abrupt changes: theory and application*. Prentice Hall Englewood Cliffs, 1993.

[10] L. Wei *et al.*, "Spectrum sensing with Gaussian approximated eigenvalue ratio based detection," in *IEEE ISWCS*, 2010, pp. 961–965.

[11] F. Penna *et al.*, "Probability of missed detection in eigenvalue ratio spectrum sensing," in *IEEE WIMOB*, 2009, pp. 117–122.

[12] E. D. Kaplan *et al.*, *Understanding GPS: principles and applications*. Artech House, 2005.